Infection dynamics of Amoebophryidae parasitoids on harmful dinoflagellates in a southern Chilean fjord dominated by diatoms

Catharina Alves-de-Souza[1,2,3,8,*], **Daniel Varela**[4], **José Luis Iriarte**[5,6,7],
Humberto E. González[1,6,7], **Laure Guillou**[2,3]

[1]**Instituto de Ciencias Marinas y Limnológicas, Universidad Austral de Chile, PO Box 567, Valdivia 5090000, Chile**
[2]**Université Pierre et Marie Curie, Paris 6, Station Biologique de Roscoff, Place Georges Teissier, Roscoff 29680, France**
[3]**Centre National de la Recherche Scientifique (CNRS), UMR 7144, Laboratoire Adaptation et Diversité en Milieu Marin, Place Georges Teissier, Roscoff 29680, France**
[4]**Centro de Investigación I-mar, Universidad de los Lagos, Casilla 557, Puerto Montt 5480000, Chile**
[5]**Instituto de Acuicultura, Universidad Austral de Chile, Los Pinos s/n, Puerto Montt 5480000, Chile**
[6]**Centro COPAS y COPAS Sur Austral, Universidad de Concepción, PO Box 160-C, Concepción 4030000, Chile**
[7]**Centro de Investigación de Ecosistemas de la Patagonia (CIEP), Coyhaique 5950000, Chile**

[8]*Present address:* **Laboratório de Ficologia, Departamento de Botânica, Museu Nacional/Universidade Federal do Rio de Janeiro, Quinta da Boa Vista S/N, São Cristóvão, Rio de Janeiro, RJ 20940-040, Brasil**

ABSTRACT: Parasitoids belonging to Amoebophryidae (Marine ALVeolate Group II or MALV II) infecting dinoflagellates were investigated in Reloncaví Fjord (southern Chile) in the austral summer 2009. Of the 12 dinoflagellate species recorded during monthly sampling, *Prorocentrum micans*, *Dinophysis acuminata*, and *Phalacroma rotundata* were infected by *Amoebophrya* spp. To assess parasitoid control of host populations, the short-term dynamics of *Amoebophrya* spp. were followed for 21 d during a bloom of *P. micans*. Host mortality induced by *Amoebophrya* spp. (% hosts killed per day) was estimated by dividing prevalence by the generation time of these parasitoids. Parasitism by *Amoebophrya* spp. was responsible for ~10% of *P. micans* mortality between 8 and 17 March. The small subunit rDNA genes of individual parasitoids infecting different host cells were sequenced, and like most environmental sequences retrieved from this ecosystem in January and February, all belonged to the MALV II Clade 4. However, as soon as the *P. micans* bloom was detected, the MALV II genetic composition changed drastically, with the detection of Clades 1, 4 (a different sub-cluster than before), 5, 6, and 12. Our results suggest that different types of parasitoids belonging to Amoebophryidae likely infect dinoflagellates in Reloncaví Fjord, offering the first demonstration of the presence of important genetic diversity in MALV II inhabiting an ecosystem where dinoflagellate hosts are not the usual dominant phytoplanktonic organisms.

KEY WORDS: *Amoebophrya* · MALV II · Parasitism · Harmful algal blooms

INTRODUCTION

The southern region of Chile (41–56° S) includes a variety of embayments, fjords, and channels characterized by high productivity. Phytoplankton abundance in this area is strongly influenced by the inter-

action between silicic acid ($Si(OH)_4$) input from freshwater discharge and the vertical entrainment of nitrate (NO_3) and orthophosphate (PO_4) from subantarctic waters (Iriarte et al. 2007, Torres et al. 2011). The constant supply of $Si(OH)_4$ from river discharge drives the high $Si(OH)_4:NO_3$ and $Si(OH)_4:PO_4$

ratios typically observed in these systems, which probably explains why diatoms are usually the predominant phytoplankton group throughout the year (Alves-de-Souza et al. 2008). It was recently suggested that drastic reductions of precipitation in southern Chile might result in lower flows from rivers and glaciers (Lara et al. 2005). This could, in turn, reduce the silicate load and cause a decline of overall fjord productivity (e.g. Rebolledo et al. 2005, Sepulveda et al. 2005). The lower ratios of $Si(OH)_4:NO_3$ and $Si(OH)_4:PO_4$ might favor species that do not require silicates, such as dinoflagellates, at the expense of diatoms (Iriarte et al. 2010). Many dinoflagellate species produce harmful algal blooms (HABs) that might be noxious to both humans and aquatic ecosystems (Smayda 1997). Thus, the frequency of HABs caused by dinoflagellates within Chilean fjords might be expected to increase. The main dinoflagellate species related to HABs in southern Chile are *Alexandrium catenella* and *Dinophysis* spp., recurrently associated with outbreaks of paralytic and diarrheic toxins, respectively (Lembeye et al. 1993, Guzmán et al. 2002, Molinet et al. 2003). Although less frequent, other dinoflagellate species, such as *Prorocentrum micans*, *Gymnodinium* cf. *chlorophorum*, and *Gymnodinium* sp., have also been recorded to form HABs, causing behavioral changes and mortality in wild and farmed aquatic resources (Lembeye & Campodónico 1984, Uribe & Ruiz 2001, Iriarte et al. 2005).

Although studies of HAB dynamics usually focus on the role of bottom-up factors, growing evidence shows the importance of biotic factors, mainly grazing and parasitism, in the demise of blooms (e.g. Calbet et al. 2003, Montagnes et al. 2008). It has recently been postulated that dinoflagellate blooms may also result from the absence of efficient pathogens in newly invaded areas (Salomon et al. 2003, Chambouvet et al. 2008), a theory known as the 'enemy release hypothesis' in terrestrial ecology (Keane & Crawley 2002). The major eukaryotic pathogens described for dinoflagellates are unicellular parasitoids belonging to the Phylum Alveolata (perkinsoids and Amoebophryidae; Park et al. 2004). Both lineages ultimately kill their hosts to accomplish their life cycles (Park et al. 2004), endowing these organisms with a typical parasitoid feature (i.e. parasitism is similar to predation by grazers in that a part of the host population will be killed). Although perkinsoids are rarely reported in environmental genetic surveys, Amoebophryidae (synonymous to Marine ALVeolate Group II or MALV II) is one of the most important eukaryotic genetic lineages retrieved from marine ecosystems

(Guillou et al. 2008). To date, Amoebophryidae is only composed of one genus, *Amoebophrya*, but this group is likely much more complex in terms of genetic diversity. Within the genus *Amoebophrya*, several species have been described as infecting a large number of dinoflagellate species (Park et al. 2004). The life cycle of these parasitoids begins with a small infective biflagellate cell (the dinospore) entering the host cell (Cachon 1964). Maturation takes 2 to 3 d and eventually leads to the death of the host and liberation of a long, worm-shaped, motile filament of biflagellate cells (the vermiform stage). Within a few hours, the vermiform stage fragments and releases hundreds of new infective dinospores (Coats & Bockstahler 1994, Coats & Park 2002), each potentially capable of infecting a novel host. Both field observations and model predictions indicate that these parasitoids have the capacity to efficiently control their dinoflagellate host populations (Cachon 1964, Coats et al. 1996, Chambouvet et al. 2008, Montagnes et al. 2008, Salomon & Stolte 2010).

Interactions between *Amoebophrya* spp. and their hosts have been assessed mainly in coastal areas of the northern hemisphere (Cachon 1964, Taylor 1968, Fritz & Nass 1992, Coats & Bockstahler 1994, Coats et al. 1996, Maranda 2001, Chambouvet et al. 2008). These studies have indicated that a moderate to high prevalence of *Amoebophrya* spp. (20 to 80%) is usually observed during annual dinoflagellate blooms in estuarine systems, where high nutrient concentrations and water mass stability favor the growth of dinoflagellates. However, recent studies in oligotrophic coastal waters of Brazil (Salomon et al. 2009) and ultra-oligotrophic waters of the Mediterranean Sea (Siano et al. 2011) have reported *Amoebophrya* spp. infections of dinoflagellates with prevalences up to 7 and 25%, respectively, suggesting that these parasitoids could also be relevant at low host concentrations.

Considering the growing occurrence of HABs caused by dinoflagellates in Chile, it is important to explore the capacity of Amoebophryidae parasitoids to successfully infect dinoflagellates in the coastal waters of this country. The main objectives of this study were (1) to evaluate the presence of these parasitoids in an ecosystem usually dominated by diatoms throughout the year and (2) to assess the capacity of Amoebophryidae to infect and control bloom-forming dinoflagellate species. The sampling strategy consisted of monthly monitoring at a fixed station in Reloncaví Fjord, an ecosystem supporting a high salmon farming activity in southern Chile, and exploring the small subunit (SSU) rDNA genetic diversity of Amoebophryidae using culture-indepen-

dent methods and the direct sequencing of infected host cells. As soon as a dinoflagellate bloom was detected, a higher frequency sampling strategy was employed to evaluate the capacity of these parasitoids to efficiently propagate infections and control their hosts. The present work constitutes the first record of Amoebophryidae infection dynamics in southern Pacific waters.

MATERIALS AND METHODS

Study area and sample collection

Situated as the closest fjord to the equator in the world, Reloncaví Fjord (~41.6° S) is one of the most representative estuarine systems in southern Chile (Fig. 1). It is ~60 km long, covers 170 km^2, and has a maximum depth of 460 m. The present study was performed in austral summer 2009 at a sampling station ~20 m deep located at the head of the fjord (41° 29′ S, 72° 18′ W). Sampling was initially performed monthly beginning in January. Dominance of *Prorocentrum micans* was observed on 8 March. Samples of this bloom were then taken every 3 d until 29 March to follow the dynamics of the infections of *P. micans* by *Amoebophrya* spp. This sampling frequency was selected considering both the average daily growth rate of dinoflagellates (0.3 d^{-1}; Smayda 1997) and the generation time of *Amoebophrya* spp. (2 to 3 d, Coats & Park 2002).

CTD (Sea Bird 19-plus) casts were used to obtain *in situ* vertical profiles of salinity, temperature, and fluorescence. Five depths were then selected for sampling. These depths were positioned (1) at the subsurface, (2) above and (3) below the pycnocline, (4) at the fluorescence maximum, and (5) at 16 m. Samples for phytoplankton, Amoebophryidae, chlorophyll *a* (chl *a*), and macronutrient analyses were collected in 3 replicates using a submergible pump (Rule 800 GPH).

Macronutrients and chl *a*

Water samples to determine macronutrient concentrations (NO$_3$, PO$_4$, Si(OH)$_4$) were collected in 50 ml polyethylene bottles and kept frozen (−20°C) until analysis using colorimetric procedures (Strickland & Parsons 1972). Water samples (50 ml) for chl *a* determination were filtered onto Whatman GF/F glass-fiber filters and frozen at −20°C until analysis. Chl *a* was extracted overnight in acetone (90%) and measured with a digital fluorometer (Turner Design Model PS-700), and its concentration (µg l^{-1}) was determined using the equation recommended by Parsons et al. (1984).

Phytoplankton counting

Samples were immediately fixed with Lugol′s solution, and quantifications were performed using the Utermöhl (1958) method under an inverted microscope (Nikon Eclipse TS100) after sedimentation in 10 ml columns. Units (cells or colonies) were quantified in random fields (Uhelinger 1964) under 20× magnification until at least 100 units (p < 0.05) were enumerated (Lund et al. 1958). For the rare species, the whole bottom of the chamber was examined at a magnification of 40×.

Amoebophryidae detection

To enumerate the Amoebophryidae dinospores and calculate *Amoebophrya* spp. prevalence (% of infected dinoflagellate hosts), 250 ml aliquots of seawater were immediately fixed after sampling with paraformaldehyde (1% final concentration), stored for 1 h
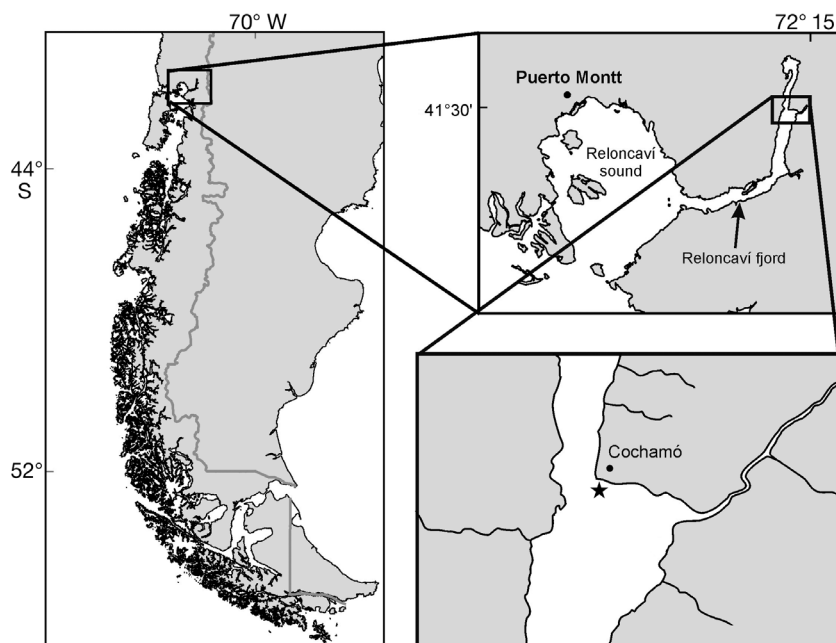

Fig. 1. Sampling station (★) in Reloncaví Fjord, southern Chile

in the dark at 4°C, and filtered onto 0.8 μm polycarbonate filters (25 mm diameter) with a vacuum pump (<200 mm Hg). The filters were then dehydrated through an ethanol series (50, 80, and 100%; 3 min each), dried briefly at room temperature, and stored at −80°C. The different Amoebophryidae life stages were detected by fluorescent *in situ* hybridization coupled with tyramide signal amplification (FISH-TSA) using the ALV01 oligonucleotide probe (5′-GCC TGC CGT GAA CAC TCT-3′) specific for Amoebophryidae (Chambouvet et al. 2008) labeled with horseradish peroxidase (Thermofisher). The FISH procedure was performed as described by Siano et al. (2011). After hybridization, the filters were covered with calcofluor (for visualization of dinoflagellate theca; 100 ng ml^{-1}) for 10 min and washed in distilled water. Then, they were mounted using antifading reagent (AF1, Citifluor) with propidium iodide (for recognition of nuclei; 10 μg ml^{-1}) and stored at 4°C until analysis.

All hybridized and stained filters were observed with an Olympus BX-51 epifluorescence microscope equipped with a 11012v2-Wide Blue filter set (ChromaTechnology) and a CCD camera (Spot-RT, Diagnostic Instruments). Cells were observed with fluorescence filter sets for calcofluor (excitation: 345 nm; emission: 455 nm), propidium iodide (excitation: 536 nm; emission: 617 nm), and fluorescein tyramide (excitation: 495 nm; emission: 520 nm). Amoebophryidae dinospores were counted at 1000× magnification in 20 randomly chosen microscopic fields. To estimate the prevalence of *Amoebophrya* spp. (% of infected hosts), dinoflagellates were counted at 20× or 40× magnification on the whole surface of the piece of filter. A specimen was considered infected when the nucleus of the parasitoid together with the probe signal were clearly identifiable in the host cell. Prevalences were considered reliable when at least 50 specimens of each dinoflagellate species were observed. Host mortality induced by *Amoebophrya*, i.e. the percentage of hosts killed per day, was estimated according to Coats & Bockstahler (1994):

$$\text{Host mortality} = \frac{Amoebophrya \text{ prevalence}}{Amoebophrya \text{ generation time}} \quad (1)$$

A generation time of 2 d was determined for *Amoebophrya* at 20°C under culture conditions (Yih & Coats 2000, Coats & Park 2002). This was adjusted to 2.85 d considering the average ambient temperature (15°C) observed during this study and a Q_{10} of 2 (Montagnes et al. 2008).

To estimate the importance of *Amoebophrya*-caused mortality for the decrease of a *Prorocentrum micans* bloom, the *in situ* growth rate (μ) of this dinoflagellate species was estimated assuming exponential growth (Guillard 1973):

$$\mu = \frac{l}{t_2 - t_1} \ln \frac{N_2}{N_1} \quad (2)$$

where μ is the growth rate (d^{-1}), and N_1 and N_2 were the abundances of *P. micans* on 8 (t_1) and 17 March (t_2), respectively.

Statistical analysis

The monthly temporal distribution of phytoplankton assemblages related to nutrient concentrations was evaluated by a canonical correspondence analysis (CCA) using CANOCO 4.5 software (ter Braak 1995). Data from sampling performed on 10 January, 14 February, and 8 and 26 March were previously transformed logarithmically (ln[x + 1]) and organized in a 'biological' matrix that included the abundance of species present in at least 10% of the samples and an 'explanatory' matrix including concentrations of silicic acid, nitrate, and orthophosphate (n = 60). Monte Carlo permutation testing (500 permutations, CANOCO 4.5) was used to determine the significance of the variables and the first 2 ordination axes.

The effect of nutrients on the short-term temporal dynamics of phytoplankton was assessed by Spearman correlation analyses (Statistica 6.0). Given the expectation of a time delay between the increase of nutrients and the phytoplankton growth response (Huppert et al. 2002), the abundances of predominant species observed at each sampling date between 11 and 29 March were correlated with the respective nutrient concentrations measured on the previous sampling date (between 8 and 26 March). Due to the strong vertical stratification usually observed in Reloncaví Fjord, correlations were established separately for each depth (n = 24) to minimize the interference of light and salinity related to the vertical variability of these variables. Similarly, because a time-delay is also expected to occur in host–parasitoid dynamics (Montagnes et al. 2008, Salomon & Stolte 2010), short-term interactions between *Prorocentrum micans* and parasitoids belonging to the Amoebophryidae were evaluated by correlating depth-integrated *P. micans* abundances from each sampling with depth-integrated numbers of dinospores and infected *P. micans* observed on the previous sampling date (n = 24). Infected *P. micans* abundances were based on the prevalence estimated by FISH and the total *P. micans* enumerated in Lugol-

stained samples. For all analyses, data were logarithmically transformed ($\ln[x + 1]$).

Amoebophryidae genetic analysis

Samples were taken by net hauling (25 µm pore size), filtered through an 80 µm mesh, and stored in ethanol (99%) at −20°C. Genetic characterization of parasitoids belonging to the Amoebophryidae was based on 5 samples obtained on 10 January, 14 February, and 8, 11, and 14 March (environmental sequences). For each sample, 100 µl of 25 µm net samples were transferred to 500 µl tubes. After centrifugation (15 min at 14 000 g at 4°C), the volume was adjusted to 10 µl. Additionally, infected dinoflagellate cells bearing a mature *Amoebophrya* trophont were individually sorted using a glass micropipette and transferred to a 500 µl tube. Two infected *Prorocentrum micans* cells collected in the Concarneau Bay (northwestern coast of France, Atlantic Ocean) on 17 May 2011 were also sequenced. DNA was extracted using a modified guanidinium isothiocyanate protocol (Chomczynski & Sacchi 2006) as described by Alves-de-Souza et al. (2011). Extraction products were used for PCR amplifications using GoTaq DNA polymerase (Promega). For environmental sequences, the SSU rDNA gene was amplified using the probe ALV01 as forward primer (5′-AGA GTG TTC ACG GCA GGC-3′) and the general eukaryotic primer 1055R as reverse (5′-ACG GCC ATG CAC CAC CCA T-3′). For isolated cells, sequences were obtained using ALV01 as forward primer and 1818R as reverse (5′-ACG GAA ACC TTG TTA CG-3′). The PCR program included a denaturation step (95°C for 5 min), followed by 35 cycles of denaturation (1 min at 95°C), hybridization (45 s at 55°C), and elongation (1 min 15 s at 72°C). The final elongation step lasted 7 min at 72°C. PCR products were cloned using the TOPO TA Cloning® kit (Invitrogen) according to manufacturer's recommendations, and selected clones were amplified by PCR following the protocol described above. PCR products were purified using the ExoSAP-IT kit (USB) following the manufacturer's recommendations and directly sequenced on an ABI Prism 3100 automatic sequencer (Applied Biosystems). The KeyDNAtools software (http://keydnatools.com) was used to remove chimeras and to assign the obtained sequences to MALV II clades as defined by Guillou et al. (2008).

Available sequences were aligned using the online package MAFFT version 6 (http://mafft.cbrc.jp/alignment/software/index.html). Environmental sequences <699 bp were not considered for phylogeny. The best nucleotide substitution model was determined using MEGA5 (Tamura et al. 2011), and a general time-reversible model was selected with a gamma distribution and invariant sites. Maximum likelihood was measured using MEGA5, and the robustness of the inferred topology was supported by bootstrap resampling (500 replicates). Gaps and missing data were completely deleted. Perkinsozoa sequences (*Parvilucifera* spp. and *Perkinsus* spp.) were used as outgroups (GenBank accession nos. X75762, AY487833, AF133909, and EU502912). The sequences obtained during this study were deposited in GenBank (accession nos. JN998202–JN998312 and JQ038241; Appendix 1).

RESULTS

Characteristics of the sampling period

The near-surface water column (0–16 m) was characterized by a 2-layer structure during the whole sampling period: the upper layer was characterized by low salinities (0.6–16) and high temperatures (14–18°C) and the lower layer by higher salinities (24–32) and lower temperatures (11–14.5°C). The result was a strongly stratified water column with a pronounced pycnocline located at 5 to 8 m (Fig. 2a,b). Strong vertical distribution was also observed for nutrients (Fig. 2c–e). The upper layer was characterized by higher concentrations of $Si(OH)_4$ (20–102 µM), whereas the lower layer generally had higher values of NO_3 (6–17 µM) and PO_4 (0.5–2 µM). The highest values of $Si(OH)_4$ and NO_3 were observed at the beginning of the sampling period in January (at 2 to 3 and 12 m, respectively), and the lowest concentrations were detected on 14 February and 11 March. After 20 March, $Si(OH)_4$ (up to 56 µM) slowly increased in the upper layer, whereas PO_4 reached the highest concentrations observed during this study (up to 3 µM) at all depths.

Fluctuations of chl *a* corresponded to different phytoplanktonic assemblages (Fig. 3a–c). The beginning of the study was characterized by moderate chl *a* concentrations, with a peak observed on 10 January at 8 m (6.6 µg l^{-1}) dominated by the diatom *Leptocylindrus minimus* (13.2×10^5 cells l^{-1}). An increase in phytoplankton biomass was observed in the subsequent months, with similar chl *a* concentrations observed on 14 February and 8 March (~12 µg l^{-1}) at 8 and 12 m, respectively. However, the specific compo-
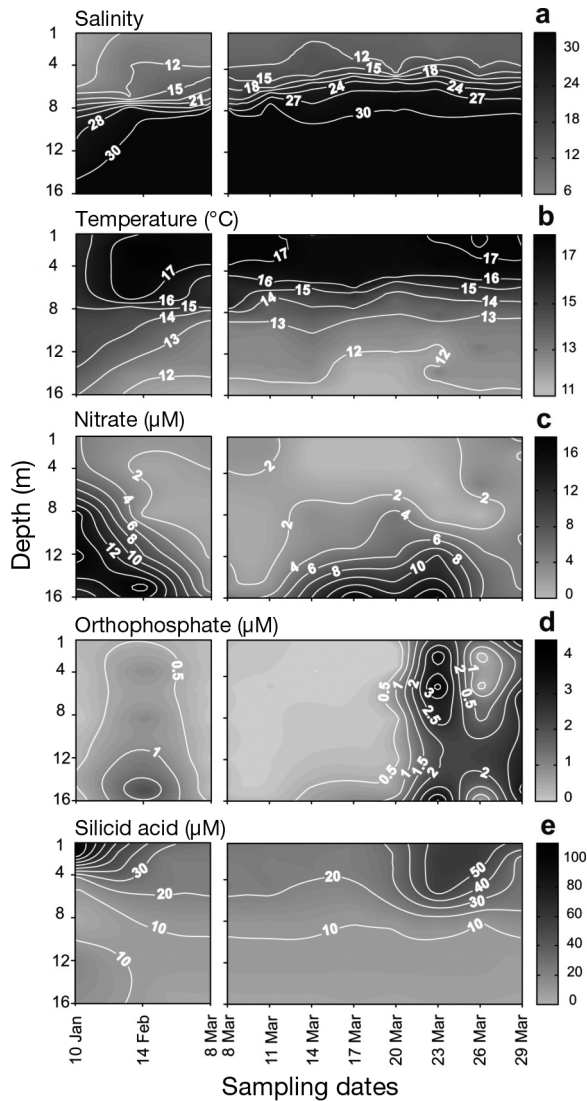
Fig. 2. Vertical and temporal distribution of (a) salinity, (b) temperature (°C), (c) nitrate (NO_3; µM), (d) orthophosphate (PO_4; µM), and (e) dissolved silicate ($Si(OH)_4$; µM) at the sampling station in Reloncaví Fjord during the austral summer 2009

Fig. 3. Temporal and vertical distribution of (a) chlorophyll a (µg l^{-1}) and abundances of (b) diatoms (× 10^5 cells l^{-1}) and (c) dinoflagellates (× 10^4 cells l^{-1}). Peaks of most abundant species are indicated by arrows. Lmin: *Leptocylindrus minimus*, Cent: small unidentified centric diatom, Skel: *Skeletonema* spp., Pmic: *Prorocentrum micans*

sition observed on these 2 sampling dates was drastically different. A small centric diatom (<5 µm) was the predominant species on 14 February (22.2 × 10^5 cells l^{-1} at 8 m), whereas the dinoflagellate *Prorocentrum micans* (10.3 × 10^4 cells l^{-1} at 12 m) dominated the phytoplankton community on 8 March. The detection of this dinoflagellate bloom started the high frequency sampling period. The *P. micans* abundance drastically decreased from 8 to 14 March (<1 × 10^4 cell l^{-1} at all depths; Fig. 3c). From 14 to 20 March, chl a values were the lowest observed during the monitoring survey (>4 µg l^{-1}), with phytoplankton assemblages mainly composed of the diatoms

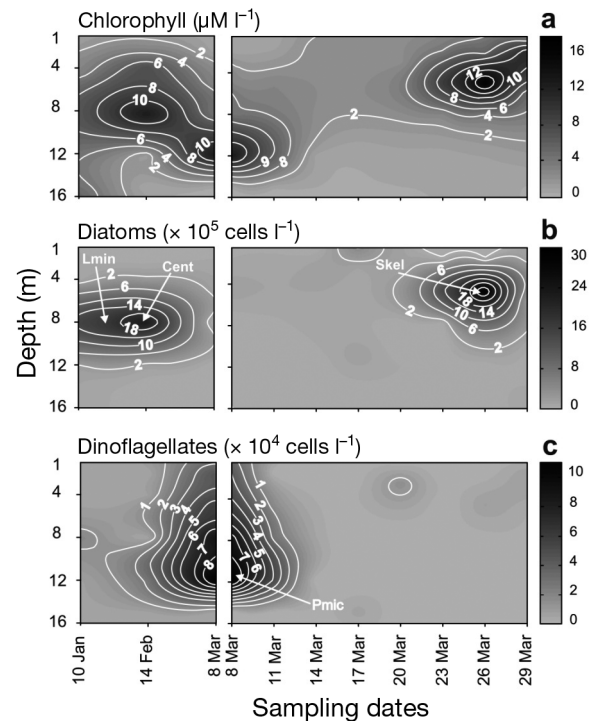*Skeletonema* spp. (>4 cells × 10^5 cells l^{-1}) and *Thalassionema nitzschioides* (<0.5 × 10^5 cells l^{-1}). Finally, the strong increase of chl a (16.5 µg l^{-1}) culminating on 26 March at 5 m was mainly induced by a bloom of *Skeletonema* spp. (29.5 × 10^5 cells l^{-1}).

The importance of nutrients on the overall composition of phytoplankton assemblages during the study was assessed by the CCA analysis applied to data collected on 10 January, 14 February, and 8 and 26 March. Together, the eigenvalues of the first 2 canonical axes (0.107 and 0.074, respectively) accounted for 77.5% of the total variance. Species and nutrients showed correlation values of 0.77 and 0.64 on the canonical Axes 1 and 2, respectively. The compositional Axis 1 (SPECIES AXIS 1) was correlated mainly with PO_4 (0.74), whereas $Si(OH)_4$ (0.40) and NO_3 (0.32) were correlated with the compositional Axis 2 (SPECIES AXIS 2), both axes being statistically significant (Monte Carlo testing, p = 0.002). The forward stepwise model indicates that these 3 nutrients were statistically significant (p = 0.002). The ordination diagram with the scores obtained is shown in Fig. 4. On Axis 1, the small centric diatom was positively correlated with PO_4 concentration, whereas on Axis 2, *Leptocylindrus minimus* and *Skeletonema* spp. were pos-
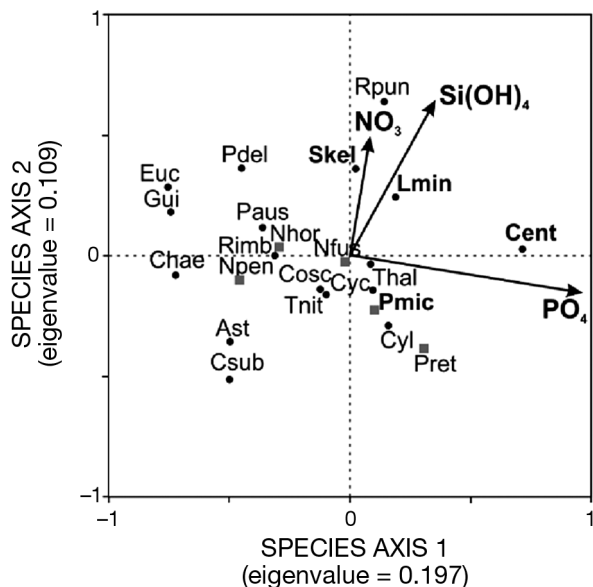
Fig. 4. Ordination diagram with the scores of species obtained in the canonical correspondence analysis related to nutrient vectors (based on data obtained on 10 January, 14 February, and 8 and 26 March). NO_3: nitrate, $Si(OH)_4$: dissolved silicate acid, PO_4: orthophosphate. ●: diatoms, ■: dinoflagellates. Most abundant species during the study in **bold**. Ast: *Asteromphalus* sp., Cent: small unidentified centric diatom, Cosc: *Coscinodiscus* spp., Csub: *Chaetoceros subtilis*, Chae: *Chaetoceros* spp., Cyc: *Cyclotella* sp., Cyl: *Cylindrotheca closterium*, Euc: *Eucampia* sp., Gui: *Guinardia delicatissima*, Lmin: *Leptocylindrus minimus*, Pdel: *Pseudo-nitzschia* spp. group *delicatissima*, Paus: *Pseudo-nitzschia* spp. group *australis*, Rimb: *Rhizosolenia imbricata*, Rpun: *Rhizosolenia pungens*, Skel: *Skeletonema*, Thal: *Thalassiosira* spp., Tnit: *Thalassionema nitzschioides*, Nfus: *Neoceratium fusum*, Nhor: *Neoceratium horridum*, Npen: *Neoceratium pentagonum*, Pmic: *Prorocentrum micans*, Pret: *Protoceratium reticulatum*

itively correlated with NO_3 and $Si(OH)_4$. *Prorocentrum micans* was also distributed on Axis 2, although it was not related to any environmental variable. For the high-frequency sampling period (8 to 29 March), a Spearman correlation analysis showed that *Skeletonema* spp. abundances were positively correlated both with the $Si(OH)_4$ (R = 0.52, p = 0.01) and PO_4 (R = 0.73, p < 0.001) levels observed 3 d before. However, no correlation was detected between the demise of *P. micans* and variation of NO_3 and PO_4 concentrations.

Infections by Amoebophryidae parasitoids

Infections, revealed by the general oligonucleotidic probe ALV01 specific for Amoebophryidae, were restricted to dinoflagellates. From a total of 12 recorded dinoflagellate taxa, only *Dinophysis acumi-*

nata, *Phalacroma rotundata*, and *Prorocentrum micans* were infected by parasitoids belonging to the Amoebophryidae (Table 1). Different life-cycle stages of parasitoids were detected by FISH using the probe ALV01 but only at depths below the halocline (Figs. 5 & 6). Dinospores (2–3 μm) were characterized by a dense nucleus occupying a large part of the cell volume (Fig. 5a). Early infections were detected in close association with the host nucleus (Fig. 5b–d). Mature trophonts showed a typical beehive configuration (Fig. 5d,f,g), indicating their affiliation to the genus *Amoebophrya*.

Infections of *Dinophysis acuminata* and *Phalacroma rotundata* were observed on 10 January and 14 February, with the highest prevalence (10%) recorded on *D. acuminata* on the first sampling date. Infections of *Prorocentrum micans* were observed on 8 March, with relatively low prevalence values (2%) observed at 12 m, together with the maximal abundance of *P. micans* (Fig. 6). An increase in prevalence was observed during the 6 subsequent days and was associated with the rapid *P. micans* bloom demise, a

Table 1. Depth-integrated abundances ($\times 10^4$ cells m^{-2}) of infected and non-infected dinoflagellate species at Reloncaví Fjord on 10 January, 14 February, and 8 March 2009. *Amoebophrya* spp. prevalence (% of infected cells) as detected by oligonucleotide probe ALV01 is shown in parentheses

|	10 January	14 February	8 March
Infected dinoflagellates			
Dinophysis	0.012	0.020	0.019
acuminata	(10%; n = 55)	(2%; n = 60)	(0%; n = 100)
Phalachroma	0.001	0.002	0.001
rotundata	(>1%; n = 20)	(0%; n = 30)	(0%; n = 25)
Prorocentrum	2.316	51.824	87.339
micans	(0%; n = 50)	(0%; n = 105)	(2%; n = 102)
Other dinoflagellates			
Neoceratium fusum	0.340	0.049	0.043
Neoceratium horridum	0.020	0.002	0.051
Neoceratium pentagonum	0.140	0.008	0.026
Dinophysis circularis	0.000	0.002	0.008
Dinophysis tripos	0.000	0.012	0.002
Dissodinium semilunula	0.220	0.008	0.003
Protoceratium reticulatum	0.000	0.295	0.226
Pyrophacus horologium	0.000	0.088	0.049
Scrippsiella cf. *trochoidea*	0.000	0.000	0.128
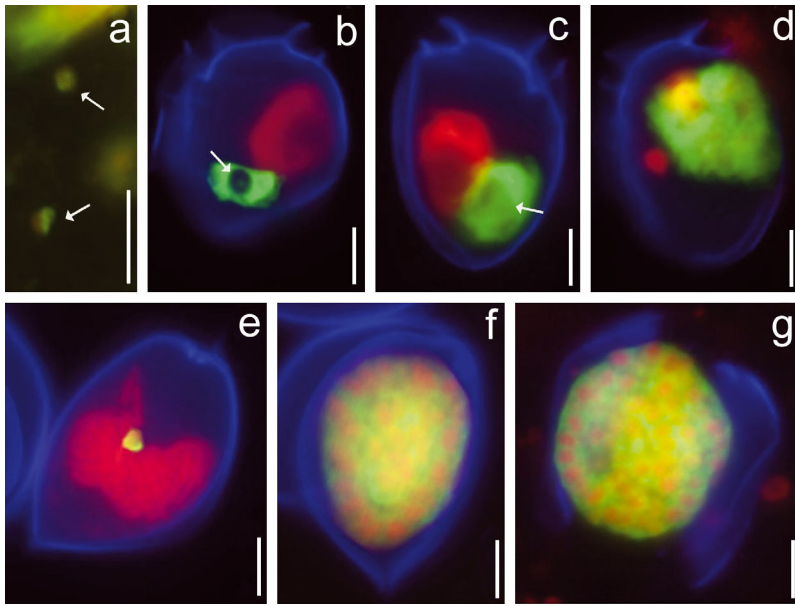
Fig. 5. *Amoebophrya* spp. life-cycle stages as detected by fluorescence *in situ* hybridization. Cell nucleus (red), dinoflagellate theca (blue), and fluorescence of probe ALV01 targeting *Amoebophrya* SSU ribosomal RNA (green) are shown. (a) Dinospores (arrows), (b) initial infection in *Dinophysis acuminata* nucleus, (c,d) intermediate infection in *Dinophysis acuminata* showing an incipient mastigocoel (arrows in b,c), (e) initial infection in *Prorocentrum micans* nucleus, and (f,g) final infection showing a mature trophont occupying the entire intracellular space of *P. micans*. Scale bars = 10 μm

greater number of infected cells on 11 March (0.47 × 10^4 cells l^{-1} at 12 m), and an important release of dinospores on 14 March (16.8 × 10^5 cells l^{-1} at 12 m). The highest prevalence (12%) was observed on 17 March at 12 m. From 14 March, *P. micans* was always detectable at relatively low abundances (equivalent to values observed during the 2 first samplings) until the end of the study. The Spearman correlation analysis showed that the dinospore abundances on each sampling date were positively correlated with the numbers of infected cells observed 3 d before (R = 0.93, p < 0.001). The estimated host mortalities due to *Amoebophrya* spp. were 0.7, 3.4, 4.2, and 4.5% on 8, 11, 14, and 17 March, respectively. On average, *Amoebophrya* spp. killed ~3.2% of the *P. micans* population each day (i.e. −0.032 d^{-1}). Considering a decrease of −0.31 d^{-1} in *P. micans* abundance during the same period, we estimated that *Amoebophrya* spp. accounted for ~10% of the total *P. micans* mortality between 8 and 17 March.

Single-cell PCR amplifications indicated that parasitoids belonging to Amoebophryidae parasitoids infecting *Dinophysis acuminata* (6 clones obtained from 2 individuals isolated in January), *Phalacroma rotundata* (5 clones obtained from 2 individuals isolated on 10 January), and *Prorocentrum micans* (1

clone resulting from 1 individual isolated on 8 March) belonged to the MALV II Clade 4, according to the classification proposed by Guillou et al. (2008) (see Appendix 1). A total of 96 environmental sequences belonging to the Amoebophryidae were obtained from the DNA extracted on 10 January, 14 February, and 8, 11, and 14 March from the planktonic communities >25 μm. Most of these sequences belonged to Clade 4 (83 sequences in total); the remaining 13 environmental sequences belonged to Clades 5, 6, and 12 (Guillou et al. 2008). Fig. 7 shows a phylogenetic analysis considering all of the sequences obtained by single-cell PCR and environmental sequences >699 bp. Although environmental sequences belonging to Clades 5 and 12 were not included in the analysis due their short length, their probable position is indicated in the phylogenetic tree. Considering bootstrap values >70%, sequences belonging to Clade 4 obtained from Reloncaví Fjord during the present study were distributed in 5 sub-clusters. Cluster A included 1 environmental sequence obtained from a sample collected on 10 January and 2 sequences of *Amoebophrya* spp. infecting *Gymnodinium instriatum* (AF472554 and HM483394) published by Gunderson et al. (2002) and Coats et al. (2010). Sequences from the infected cells of *D. acuminata* and *P. rotundata* were affiliated to Sub-clusters B, C, and D. Sub-cluster E was exclusively formed by environmental sequences retrieved on 14 March and also included 2 sequences of *Amoebophrya* spp. infecting *P. micans* (AY208893) and *Ceratium tripos* (AY208893) published by Kim et al. (2008). Although the 2 infected *P. micans* cells (JN998214 and JQ038241) collected in Concarneau Bay also belonged to Clade 4, they were grouped in a sub-cluster separate from the sequences obtained from Reloncaví Fjord.

DISCUSSION

Evolution of phytoplankton assemblages

Prorocentrum micans is a common species in summer phytoplankton assemblages in southern Chile, although it is usually observed at low abundances
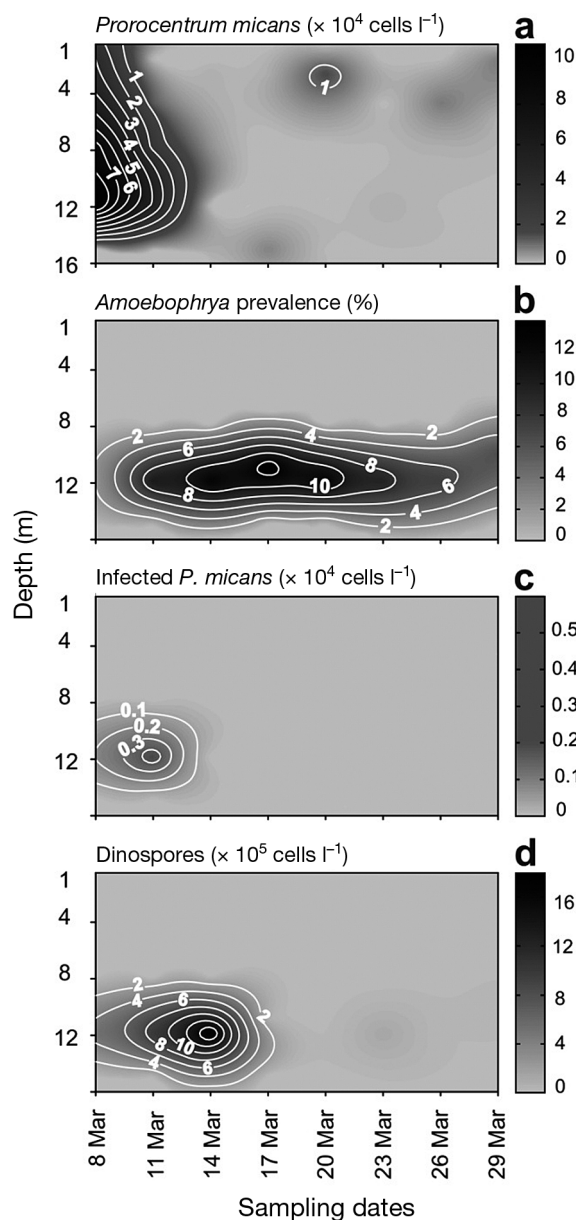
Fig. 6. Vertical and temporal dynamics of infection by parasitoids belonging to the Amoebophryidae on *Prorocentrum micans* observed between 8 and 29 March 2009. (a) *P. micans* abundances ($\times 10^4$ cells l^{-1}), (b) *Amoebophrya* prevalences (%) on *P. micans* (c), number of infected *P. micans* ($\times 10^4$ cells l^{-1}), and (d) concentration of dinospores ($\times 10^5$ cells l^{-1})

(<100 cells l^{-1}, C. Alves-de-Souza unpubl. data). The last bloom reported in the study area was in March 1983, with relatively high abundances (3.8 $\times 10^7$ cells l^{-1}; Lembeye & Campodónico 1984) covering an extensive geographical area including Reloncaví Fjord and part of Reloncaví Sound (both indicated in Fig. 1). The magnitude and geographical extension of the *P. micans* bloom observed in March 2009 was apparently similar to that observed 26 yr before

(A. Clément pers. comm.). Maximum *P. micans* abundances occurred simultaneously with the lowest Si(OH)$_4$ levels observed during the present study, whereas diatom blooms were positively related to high Si(OH)$_4$:NO$_3$ periods. The relative concentrations of Si(OH)$_4$ and NO$_3$ have been highlighted as the main factor determining phytoplankton composition in the fjords of southern Chile (Alves-de-Souza et al. 2008, Torres et al. 2011), with low Si(OH)$_4$:NO$_3$ ratios favoring the development of non-diatom blooms (Iriarte et al. 2001, 2007).

Parasitoid and host diversity

Although 12 species of dinoflagellates were identified, only 3 (*Dinophysis acuminata*, *Phalacroma rotundata*, and *Prorocentrum micans*) were infected by parasitoids belonging to the Amoebophryidae. Despite that, and taking into account the restricted spatial scale considered in the present study, parasitoids belonging to the Amoebophryidae were genetically diverse, as they were represented by 5 different clades. Clade 5, 6, and 12 are only known from environmental sequences. Sequences belonging to these clades are probably widely distributed (detected to date in the North Sea, the northern French coast, the Indian Ocean, the Sargasso Sea, and the Mediterranean Sea; Guillou et al. 2008). Clade 4 has been reported to infect *P. micans* from Chesapeake Bay, USA (AY208893; Kim et al. 2008), and Concarneau Bay, on the northwestern coast of France (JN998213 and JQ038241). This clade was also reported to infect other dinoflagellate species, such as *Alexandrium affine*, *Ceratium tripos*, *Ceratium lineatum* (AY775284, AY208892, and AY260467; Kim et al. 2008), and *Gymnodinium instriatum* (AF472554 and HM483394; Gunderson et al. 2002, Coats et al. 2010, respectively). Finally, Clade 1 was also described to infect dinoflagellates such as *Heterocapsa rotundata* (Chambouvet et al. 2008), *Prorocentrum minimum* (AY208894), and *Karlodinium veneficum* (AF472553; Gunderson et al. 2002). From these examples, it seems that the host-specificity of Amoebophryidae parasitoids was not linked to its genetic filiations based upon the SSU rRNA gene (Gunderson et al. 2002, Kim et al. 2008).

Amoebophrya spp. belonging to Clade 4 were confirmed to infect *Dinophysis acuminata*, *Phalacroma rotundata*, and *Prorocentrum micans* based on single-cell PCR. However, phylogenetic analyses revealed that these host species were, in fact, infected by *Amoebophrya* spp. belonging to different sub-
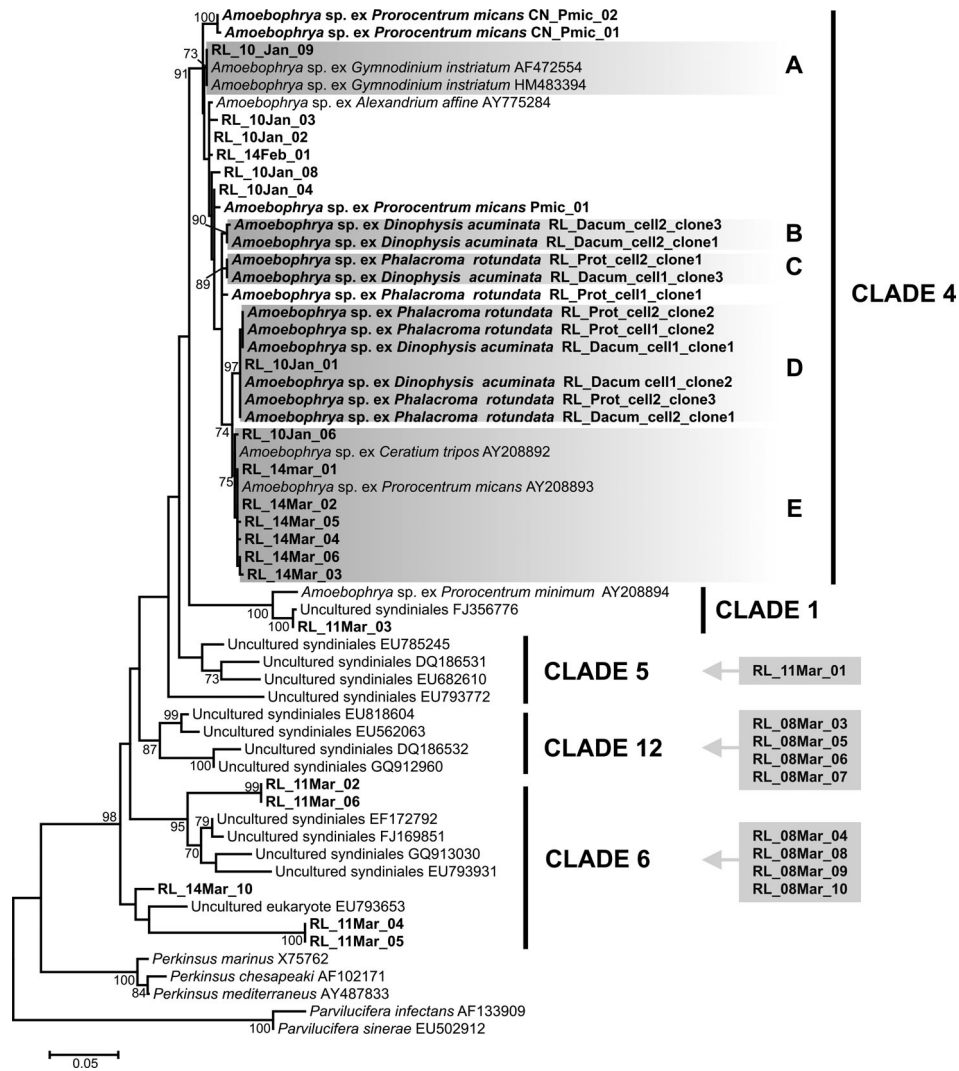
Fig. 7. Phylogeny of parasitoids belonging to the Amoebophryidae using maximum likelihood (ML) analyses of SSU rDNA genes. Sequences obtained in this study are in **bold** (for GenBank numbers, see Appendix 1). ML bootstrap values (>70%) are reported at the nodes. Clades 1, 4, 5, 6, and 12 were recognized according to Guillou et al. (2008). Subclusters (A–E) within Clade 4 with bootstrap values >70% are highlighted in gray. The probable positions of environmental sequences <699 bp belonging to Clades 5, 6, and 12 are indicated by arrows and gray boxes. Scale bar corresponds to 0.05% divergence

clusters (i.e. different genotypes). Different types of sequences were also obtained from the same host cell, both for *D. acuminata* and *P. rotundata*. Infections in the same dinoflagellate host (*Dinophysis norvegica*) by *Amoebophrya* spp. belonging to different genotypes have been previously reported from the Baltic Sea and the North Sea (Salomon et al. 2003). However, this is the first report of different *Amoebophrya* spp. genotypes infecting the same dinoflagellate individual. Similar results were found by Bachvaroff et al. (2012), who pointed out that individual tintinnid ciliates are frequently infected by different genotypes of *Euduboscquella* spp. (Syndiniales, MALV Group I). Although parasitoid populations are

usually considered to be homogeneous groups, intraspecific genetic diversity determines that some individuals are more aggressive when infecting hosts than others (Combes 2005). This has been demonstrated in culture experiments for the perkinsoid *Parvilucifera sinerae* infecting the dinoflagellate *Alexandrium minutum* (Figueroa et al. 2010) and for chytrid fungi infecting freshwater diatoms (Ibelings et al. 2004). Host-parasitoid interactions are characterized by an 'arms race' between host and parasitoid populations, and this, in turn, results in the rapid co-evolution between partners and/or cyclic variability in parasitic control (the Red Queen hypothesis; Van Valen 1973). As a consequence, a long coexistence of

parasitoid and host populations will be reflected in higher intraspecific genetic diversity. This would help to explain, for example, the drastic change in the genetic composition of environmental sequences observed on 8 and 14 March during the present study and the fact that the sequences of *Amoebophrya* spp. infecting *P. micans* from Reloncaví Fjord and those from other geographic areas were distributed in different sub-clusters.

Host–Amoebophryidae dynamics

The observed *Prorocentrum micans* and *Amoebophrya* dynamic conforms to what has previously been reported for Amoebophryidae (e.g. Coats & Park 2002, Chambouvet et al. 2008, Salomon & Stolte 2010). Maximal host abundances were followed by increased parasitoid prevalence and the consequent release of dinospores that reached their maximal density 6 d after the host peak. This burst of dinospores declined in 3 d, an observation that correlates with the short survival time of dinospores observed in culture (Coats & Park 2002). Estimations of the host mortality induced by *Amoebophrya* spp. indicated that ~10% of the *P. micans* population was killed by these parasitoids between 8 and 17 March. Although this value only partially explains the decrease of *P. micans* abundance observed for the same period (94%), our results indicate that parasitism by organisms belonging to the Amoebophryidae likely constituted an important loss for its dinoflagellate host during the study period.

The strength of infection by *Amoebophrya* spp. is often related to the abundance of its dinoflagellate hosts in natural systems (Park et al. 2004). In this sense, the prevalences observed in *Dinophysis acuminata* and *Phalacroma rotundata* (<10%) were consistent with their low abundances and in accordance with the previous records of *Amoebophrya* spp. infections of *Dinophysis* species (Fritz & Nass 1992, Gisselson et al. 2002, Salomon et al. 2009). However, prevalences were unexpectedly low for *Prorocentrum micans*, with a maximum of 12% observed on 17 March. Because *P. micans* abundances were of the same order of magnitude as during other dinoflagellate blooms in which high *Amoebophrya* spp. prevalences (30 to 80%) have been recorded (Nishitani et al. 1985, Coats et al. 1996, Chambouvet et al. 2008), we expected to find a higher percentage of infected cells during the present study. Nevertheless, culture studies (Yih & Coats 2000, Coats & Park 2002) and mathematical simula-

tions (Salomon & Stolte 2010) have demonstrated that the maximal prevalence of *Amoebophrya* spp. depends on the ratio between host and dinospores rather than host density. Using equations given by Salomon & Stolte (2010) and considering a generation time of 2.85 d, parasitoid mortality of 0.5 d^{-1} (Coats & Park 2002), and the conditions observed on 8 March (parasitoid prevalences, host and dinospore abundances), on 11 March, we should have observed prevalences similar to those found by Chambouvet et al. (2008) for *Amoebophrya* spp. infecting *Alexandrium minutum* (~40%). Grazing by ciliates on dinospores has been shown to strongly suppress *Amoebophrya* infections under natural conditions (Johansson & Coats 2002). Unfortunately, we have no antecedents regarding ciliate abundances during the studied period, but considering that the number of dinospores actually increased from 8 to 11 March, it seems that dinospore mortality (by grazing or other sources) was not the main factor determining *Amoebophrya* spp. success during this 3 d period. Alternatively, because nutrients can have a positive effect on the infective success and longevity of dinospores under culture conditions (Yih & Coats 2000), it is possible that low NO_3 and PO_4 concentrations could have had an adverse effect on the quality of the dinospores produced.

The present study demonstrated for the first time that parasitoids belonging to the Amoebophryidae could be genetically diversified, even in ecosystems where their dinoflagellate hosts are not the predominant phytoplankton group. Although *Prorocentrum micans* is a common species in southern Chile, it usually occurs at very low abundances, and the formation of blooms is rare. According to Chambouvet et al. (2008), the capacity of parasitoids to control host populations is diminished when the excessive growth of a rare species is stimulated by environmental changes, when resistant host populations may actually be favored. This would be particularly relevant in ecosystems like the Chilean fjords, in which climate changes may favor increased dinoflagellate HABs.

government) and by the French ANR Paralex ('The Sixth Extinction'). Additional support for her PhD thesis was provided by the Centro de Investigación de Ecosistemas de la Patagonia (CIEP).

LITERATURE CITED

Alves-de-Souza C, González MT, Iriarte JL (2008) Functional groups in marine phytoplankton assemblages dominated by diatoms in fjords of southern Chile. J Plankton Res 30:1233–1243

Alves-de-Souza C, Cornet C, Nowaczyk A, Gasparini S, Skovgaard A, Guillou L (2011) *Blastodinium* spp. infect copepods in the ultra-oligotrophic marine waters of the Mediterranean Sea. Biogeosciences 8:2125–2136

Bachvaroff TR, Kim S, Guillou L, Delwiche C, Coats DW (2012) Molecular diversity of the Syndinian genus *Euduboscquella* based on single-cell PCR analysis. Appl Environ Microbiol 78:334–345

Cachon J (1964) Contribution à l'étude des péridiniens parasites. Cytologie, cycles évolutifs. Ann Sci Nat Zool 6: 1–158

Calbet A, Vaqué D, Felipe J, Vila M, Sala MM, Alcaraz M, Estrada M (2003) Relative grazing impact of microzooplankton and mesozooplankton on a bloom of the toxic dinoflagellate *Alexandrium minutum*. Mar Ecol Prog Ser 259:303–309

Chambouvet A, Morin P, Marie D, Guillou L (2008) Control of toxic marine dinoflagellate blooms by serial parasitic killers. Science 322:1254–1257

Chomczynski P, Sacchi N (2006) The single-step method of RNA isolation by acid guanidinium thiocyanate-phenol-chloroform extraction: twenty-something years on. Nat Protoc 1:581–585

Coats DW, Bockstahler KR (1994) Occurrence of the parasitic dinoflagellate *Amoebophrya ceratii* in Chesapeake Bay populations of *Gymnodinium sanguineum*. J Eukaryot Microbiol 41:586–593

Coats DW, Park MG (2002) Parasitism of photosynthetic dinoflagellates by three strains of *Amoebophrya* (Dinophyta): parasite survival, infectivity, generation time, and host specificity. J Phycol 38:520–528

Coats DW, Adam EJ, Gallegos CL, Hedrick S (1996) Parasitism of photosynthetic dinoflagellates in a shallow subestuary of Chesapeake Bay, USA. Aquat Microb Ecol 11:1–9

Coats DW, Kim S, Bachvaroff TR, Handy SM, Delwiche CF (2010) *Tintinnophagus acutus* n. g., n. sp. (Phylum Dinoflagellata), an ectoparasite of the ciliate *Tintinnopsis cylindrica* Daday 1887, and its relationship to *Duboscquodinium collini* Grasse 1952. J Eukaryot Microbiol 57: 468–482

Combes C (2005) The art of being a parasite. The University of Chicago Press, Chicago

Figueroa RI, Garcés E, Camp J (2010) Reproductive plasticity and local adaptation in the host-parasite system formed by the toxic *Alexandrium minutum* and the dinoflagellate parasite *Parvilucifera sinerae.* Harmful Algae 10:56–63

Fritz L, Nass M (1992) Development of two endoparasitic dinoflagellate *Ameobophrya ceratii* within host dinoflagellate species. J Phycol 28:312–320

Gisselson LA, Carlsson P, Granéli E, Pallon J (2002) *Dinophysis* blooms in the deep euphotic zone of the Baltic Sea: Do they grow in the dark? Harmful Algae 1:401–418

Guillard R (1973) Methods for microflagellates and nannoplankton. In: Stein J (ed) Handbook of phycological methods: culture methods and growth measurements. Cambridge University Press, Cambridge, p 69–85

Guillou L, Viprey M, Chambouvet A, Welsh RM and others (2008) Widespread occurrence and genetic diversity of marine parasitoids belonging to Syndiniales (Alveolata). Environ Microbiol 10:3349–3365

Gunderson JH, John SA, Boman WC, Coats DW (2002) Multiple strains of the parasitic dinoflagellate *Amoebophrya* exist in Chesapeake Bay. J Eukaryot Microbiol 49: 469–474

Guzmán L, Pacheco H, Pizarro G, Alarcón C (2002) *Alexandrium catenella* y veneno paralizante de los mariscos en Chile. In: Sar EA, Ferrario ME, Reguera B (eds) Floraciones algales nocivas en el Cono Sur Americano. Instituto Español de Oceanografía, Vigo, p 235–256

Huppert A, Blasius B, Stone S (2002) A model of phytoplankton blooms. Am Nat 159:156–171

Ibelings BW, De Bruin A, Kagami M, Rijkeboer M, Brehm M, Van Donk E (2004) Host parasite interactions between freshwater phytoplankton and chytrid fungi. J Phycol 40: 437–453

Iriarte JL, Kusch A, Ruiz M (2001) Phytoplankton biomass in the sub-Antarctic area of the Straits of Magellan (53° S), Chile during spring-summer 1997–1998. Polar Biol 24: 154–162

Iriarte JL, Quiñones L, González RR (2005) Relationship between biomass and enzymatic activity of a bloom-forming dinoflagellate (Dinophyceae) in southern Chile (41° S): a field approach. J Plankton Res 27:159–166

Iriarte JL, González HE, Liu KK, Rivas C, Valenzuela C (2007) Spatial and temporal variability of chlorophyll and primary productivity in surface waters of southern Chile (41.5–43° S). Estuar Coast Shelf Sci 74:471–480

Iriarte JL, González HE, Nahuelhual L (2010) Patagonian fjord ecosystems in southern Chile as a highly vulnerable region: problems and needs. Ambio 39:463–466

Johansson M, Coats DW (2002) Ciliate grazing on the parasite *Amoebophrya* sp. decreases infection of the red-tide dinoflagellate *Akashiwo sanguinea.* Aquat Microb Ecol 28:69–78

Keane RM, Crawley MJ (2002) Exotic plant invasions and the enemy release hypothesis. Trends Ecol Evol 17: 164–170

Kim S, Park MG, Kim KY, Kim CH, Yih W, Park JS, Coats DW (2008) Genetic diversity of parasitic dinoflagellates in the genus *Amoebophrya* and its relationship to parasite biology and biogeography. J Eukaryot Microbiol 55: 1–8

Lara A, Urrutia R, Luckman BH, Soto D and others (2005) The potential use of tree-rings to reconstruct streamflow and estuarine salinity in the Valdivian Rainforest ecoregion. Dendrochronologia 22:155–161

Lembeye G, Campodónico I (1984) First record bloom of the dinoflagellate *Prorocentrum micans.* Bot Mar 27:491–493

Lembeye G, Yasumoto T, Zhao J, Fernández R (1993) DSP outbreak in Chilean Fjords. In: Smayda TJ, Shimizu Y (eds) Toxic phytoplankton blooms in the sea. Elsevier, Amsterdam, p 525–529

Lund JWG, Kipling C, Lecren ED (1958) The inverted microscope method of estimating algal number and the statistical basis of estimating by counting. Hydrobiologia 11: 143–170

Maranda L (2001) Infection of *Prorocentrum minimum* (Dinophyceae) by the parasite *Amoebophrya* sp. (Dinoflagellea). J Phycol 37:245–248

Molinet C, Lafon A, Lembeye G, Moreno C (2003) Spatial and temporal distribution patterns of blooms of *Alexandrium catenella* (Whedon & Kofoid) Balech 1985, on inland seas of northwest Patagonia, Chile (in Spanish with English Abstract). Rev Chil Hist Nat 76:681–698

Montagnes DJS, Chambouvet A, Guillou L, Fenton A (2008) Responsibility of microzooplankton and parasite pressure for the demise of toxic dinoflagellate blooms. Aquat Microb Ecol 53:211–225

Nishitani L, Erickson G, Chew KK (1985) Role of the parasitic dinoflagellate *Amoebophrya ceratii* in control of *Gonyaulax catenella* populations. In: Anderson DM, White AW, Baden DG (eds) Toxic dinoflagellates. Elsevier, New York, NY, p 225–232

Park MG, Yih W, Coats DW (2004) Parasites and phytoplankton, with special emphasis on dinoflagellate infections. J Eukaryot Microbiol 51:145–155

Parsons TR, Maita Y, Lalli CM (1984) A manual of chemical and biological methods for seawater analysis. Pergamon Press, Oxford

Rebolledo L, Lange C, Figueroa D, Pantoja S, Muñoz P, Castro R (2005) 20th century fluctuations in the abundance of siliceous microorganisms preserved in the sediments of the Puyuhuapi channel. Rev Chil Hist Nat 78:469–488

Salomon PS, Stolte W (2010) Predicting the population dynamics in *Amoebophrya* parasitoids and their dinoflagellate hosts using a mathematical model. Mar Ecol Prog Ser 419:1–10

Salomon PS, Janson S, Granéli E (2003) Multiple species of the dinophagous dinoflagellate genus *Amoebophrya* infect the same host species. Environ Microbiol 5: 1046–1052

Salomon PS, Granéli E, Neves MHCB, Rodriguez EG (2009) Infection by *Amoebophrya* spp. parasitoids of dinoflagellates in a tropical marine coastal area. Aquat Microb Ecol 55:143–153

Sepulveda J, Pantoja S, Hughen K, Lange C and others (2005) Fluctuations in export productivity over the last century from sediments of a southern Chilean fjord (44° S). Estuar Coast Shelf Sci 65:587–600

Siano R, Alves-de-Souza C, Foulon E, Bendif EIM, Simon N, Guillou L, Not F (2011) Distribution and host diversity of Amoebophryidae parasites across oligotrophic waters of the Mediterranean Sea. Biogeosciences 8:267–278

Smayda TJ (1997) Harmful algal blooms: their ecophysiology and general relevance to phytoplankton blooms in the sea. Limnol Oceanogr 42:1137–1153

Strickland JDH, Parsons TR (1972) A practical handbook of seawater analysis. Fisheries Research Board of Canada, Ottawa

Tamura K, Peterson D, Peterson N, Stecher G, Nei M, Kumar S (2011) MEGA5: molecular evolutionary genetics analysis using maximum likelihood, evolutionary distance, and maximum parsimony methods. Mol Biol Evol 28: 2731–2739

Taylor FJR (1968) Parasitism of the toxin-producing dinoflagellate *Gonyaulax catenella* by the endoparasitic dinoflagellate *Amoebophrya ceratii*. J Fish Res Board Can 25:2241–2245

ter Braak CJ (1995) Ordination. In: Jongman RH, ter Braak CJ, Van Tongeren OF (eds) Data analysis and community and landscape ecology. Cambridge University Press, Cambridge, p 91–73

Torres R, Frangópulos M, Hamamé M, Montecino V and others (2011) Nitrate to silicate ratio variability and the composition of micro-phytoplankton blooms in the inner-fjord of Seno Ballena (Strait of Magellan, 54° S). Cont Shelf Res 31:244–253

Uhelinger V (1964) Étude statistique des methods de dénobrement planctonique. Arch Sci 17:121–223

Uribe JC, Ruiz M (2001) *Gymnodinium* brown tide in the Magellanic fjords, southern Chile. Rev Biol Mar Oceanogr 36:155–164

Utermöhl H (1958) Zur Vervollkommnung der quantitativen Phytoplankton-Methodik. Mitt Int Ver Theor Angew Limnol 9:1–38

Van Valen L (1973) A new evolutionary law. Evol Theory 1: 1–30

Yih W, Coats DW (2000) Infection of *Gymnodinium sanguineum* by the dinoflagellate *Amoebophrya* sp.: effect of nutrient environment on parasite generation time, reproduction, and infectivity. J Eukaryot Microbiol 47: 504–510

Appendix 1. Complete list of obtained sequences. ES = environmental samples, SC = single cells

GenBank number	ID	Organism	Host	Source	Geographical area	MALV II clade
JN998202	RL_Dacum_cell1_clone01	*Amoebophrya* sp.	*Dinophysis acuminata*	SC	Reloncaví Fjord, Chile	4
JN998203	RL_Dacum_cell1_clone02	*Amoebophrya* sp.	*D. acuminata*	SC	Reloncaví Fjord, Chile	4
JN998204	RL_Dacum_cell1_clone 03	*Amoebophrya* sp.	*D. acuminata*	SC	Reloncaví Fjord, Chile	4
JN998205	RL_Dacum_cell2_clone 01	*Amoebophrya* sp.	*D. acuminata*	SC	Reloncaví Fjord, Chile	4
JN998206	RL_Dacum_cell2_clone 02	*Amoebophrya* sp.	*D. acuminata*	SC	Reloncaví Fjord, Chile	4
JN998207	RL_Dacum_cell2_clone 03	*Amoebophrya* sp.	*D. acuminata*	SC	Reloncaví Fjord, Chile	4
JN998208	RL_Prot_cell1_clone 01	*Amoebophrya* sp.	*Phalachroma rotundata*	SC	Reloncaví Fjord, Chile	4
JN998209	RL_Prot_cell1_clone 02	*Amoebophrya* sp.	*P. rotundata*	SC	Reloncaví Fjord, Chile	4
JN998210	RL_Prot_cell2_clone 01	*Amoebophrya* sp.	*P. rotundata*	SC	Reloncaví Fjord, Chile	4
JN998211	RL_Prot_cell2_clone 02	*Amoebophrya* sp.	*P. rotundata*	SC	Reloncaví Fjord, Chile	4
JN998212	RL_Prot_cell2_clone 03	*Amoebophrya* sp.	*P. rotundata*	SC	Reloncaví Fjord, Chile	4
JN998213	RL_Pmic_01	*Amoebophrya* sp.	*Prorocentrum micans*	SC	Reloncaví Fjord, Chile	4
JQ038241	CN_Pmic_01	*Amoebophrya* sp.	*P. micans*	SC	Concarneau Bay, France	4
JN998214	CN_Pmic_02	*Amoebophrya* sp.	*P. micans*	SC	Concarneau Bay, France	4
JN998215	RL_10Jan_01	Uncultured Syndiniales	Unknown	ES	Reloncaví Fjord, Chile	4
JN998216	RL_10Jan_02	Uncultured Syndiniales	Unknown	ES	Reloncaví Fjord, Chile	4
JN998217	RL_10Jan_03	Uncultured Syndiniales	Unknown	ES	Reloncaví Fjord, Chile	4
JN998218	RL_10Jan_04	Uncultured Syndiniales	Unknown	ES	Reloncaví Fjord, Chile	4
JN998219	RL_10Jan_05	Uncultured Syndiniales	Unknown	ES	Reloncaví Fjord, Chile	4
JN998220	RL_10Jan_06	Uncultured Syndiniales	Unknown	ES	Reloncaví Fjord, Chile	4
JN998221	RL_10Jan_07	Uncultured Syndiniales	Unknown	ES	Reloncaví Fjord, Chile	4
JN998222	RL_10Jan_08	Uncultured Syndiniales	Unknown	ES	Reloncaví Fjord, Chile	4
JN998223	RL_10Jan_09	Uncultured Syndiniales	Unknown	ES	Reloncaví Fjord, Chile	4
JN998224	RL_10Jan_10	Uncultured Syndiniales	Unknown	ES	Reloncaví Fjord, Chile	4
JN998225	RL_14Feb_01	Uncultured Syndiniales	Unknown	ES	Reloncaví Fjord, Chile	4
JN998226	RL_14Feb_02	Uncultured Syndiniales	Unknown	ES	Reloncaví Fjord, Chile	4
JN998227	RL_14Feb_03	Uncultured Syndiniales	Unknown	ES	Reloncaví Fjord, Chile	4
JN998228	RL_14Feb_04	Uncultured Syndiniales	Unknown	ES	Reloncaví Fjord, Chile	4
JN998229	RL_14Feb_05	Uncultured Syndiniales	Unknown	ES	Reloncaví Fjord, Chile	4
JN998230	RL_14Feb_06	Uncultured Syndiniales	Unknown	ES	Reloncaví Fjord, Chile	4
JN998231	RL_14Feb_07	Uncultured Syndiniales	Unknown	ES	Reloncaví Fjord, Chile	4
JN998232	RL_14Feb_08	Uncultured Syndiniales	Unknown	ES	Reloncaví Fjord, Chile	4
JN998233	RL_14Feb_09	Uncultured Syndiniales	Unknown	ES	Reloncaví Fjord, Chile	4
JN998234	RL_14Feb_10	Uncultured Syndiniales	Unknown	ES	Reloncaví Fjord, Chile	4
JN998235	RL_14Feb_11	Uncultured Syndiniales	Unknown	ES	Reloncaví Fjord, Chile	4
JN998236	RL_14Feb_12	Uncultured Syndiniales	Unknown	ES	Reloncaví Fjord, Chile	4
JN998237	RL_14Feb_13	Uncultured Syndiniales	Unknown	ES	Reloncaví Fjord, Chile	4
JN998238	RL_14Feb_14	Uncultured Syndiniales	Unknown	ES	Reloncaví Fjord, Chile	4
JN998239	RL_14Feb_15	Uncultured Syndiniales	Unknown	ES	Reloncaví Fjord, Chile	4
JN998240	RL_14Feb_16	Uncultured Syndiniales	Unknown	ES	Reloncaví Fjord, Chile	4
JN998241	RL_14Feb_17	Uncultured Syndiniales	Unknown	ES	Reloncaví Fjord, Chile	4
JN998242	RL_14Feb_18	Uncultured Syndiniales	Unknown	ES	Reloncaví Fjord, Chile	4
JN998243	RL_14Feb_19	Uncultured Syndiniales	Unknown	ES	Reloncaví Fjord, Chile	4
JN998244	RL_14Feb_20	Uncultured Syndiniales	Unknown	ES	Reloncaví Fjord, Chile	4
JN998245	RL_14Feb_21	Uncultured Syndiniales	Unknown	ES	Reloncaví Fjord, Chile	4
JN998246	RL_14Feb_22	Uncultured Syndiniales	Unknown	ES	Reloncaví Fjord, Chile	4
JN998247	RL_14Feb_23	Uncultured Syndiniales	Unknown	ES	Reloncaví Fjord, Chile	4
JN998248	RL_14Feb_24	Uncultured Syndiniales	Unknown	ES	Reloncaví Fjord, Chile	4
JN998249	RL_14Feb_25	Uncultured Syndiniales	Unknown	ES	Reloncaví Fjord, Chile	4
JN998250	RL_14Feb_26	Uncultured Syndiniales	Unknown	ES	Reloncaví Fjord, Chile	4
JN998251	RL_14Feb_27	Uncultured Syndiniales	Unknown	ES	Reloncaví Fjord, Chile	4
JN998252	RL_14Feb_28	Uncultured Syndiniales	Unknown	ES	Reloncaví Fjord, Chile	4
JN998253	RL_14Feb_29	Uncultured Syndiniales	Unknown	ES	Reloncaví Fjord, Chile	4
JN998254	RL_14Feb_30	Uncultured Syndiniales	Unknown	ES	Reloncaví Fjord, Chile	4
JN998255	RL_14Feb_31	Uncultured Syndiniales	Unknown	ES	Reloncaví Fjord, Chile	4
JN998256	RL_14Feb_32	Uncultured Syndiniales	Unknown	ES	Reloncaví Fjord, Chile	4
JN998257	RL_11Mar_01	Uncultured Syndiniales	Unknown	ES	Reloncaví Fjord, Chile	5
JN998258	RL_11Mar_02	Uncultured Syndiniales	Unknown	ES	Reloncaví Fjord, Chile	6

Appendix 1 (continued)

GenBank number	ID	Organism	Host	Source	Geographical area	MALV II clade
JN998259	RL_11Mar_03	Uncultured Syndiniales	Unknown	ES	Reloncaví Fjord, Chile	1
JN998260	RL_11Mar_04	Uncultured Syndiniales	Unknown	ES	Reloncaví Fjord, Chile	6
JN998261	RL_11Mar_05	Uncultured Syndiniales	Unknown	ES	Reloncaví Fjord, Chile	6
JN998262	RL_11Mar_06	Uncultured Syndiniales	Unknown	ES	Reloncaví Fjord, Chile	6
JN998263	RL_14Mar_01	Uncultured Syndiniales	Unknown	ES	Reloncaví Fjord, Chile	4
JN998264	RL_14Mar_02	Uncultured Syndiniales	Unknown	ES	Reloncaví Fjord, Chile	4
JN998265	RL_14Mar_03	Uncultured Syndiniales	Unknown	ES	Reloncaví Fjord, Chile	4
JN998266	RL_14Mar_04	Uncultured Syndiniales	Unknown	ES	Reloncaví Fjord, Chile	4
JN998267	RL_14Mar_05	Uncultured Syndiniales	Unknown	ES	Reloncaví Fjord, Chile	4
JN998268	RL_14Mar_06	Uncultured Syndiniales	Unknown	ES	Reloncaví Fjord, Chile	4
JN998269	RL_14Mar_07	Uncultured Syndiniales	Unknown	ES	Reloncaví Fjord, Chile	4
JN998270	RL_14Mar_08	Uncultured Syndiniales	Unknown	ES	Reloncaví Fjord, Chile	4
JN998271	RL_14Mar_09	Uncultured Syndiniales	Unknown	ES	Reloncaví Fjord, Chile	4
JN998272	RL_14Mar_10	Uncultured Syndiniales	Unknown	ES	Reloncaví Fjord, Chile	6
JN998273	RL_14Mar_11	Uncultured Syndiniales	Unknown	ES	Reloncaví Fjord, Chile	4
JN998274	RL_14Mar_12	Uncultured Syndiniales	Unknown	ES	Reloncaví Fjord, Chile	4
JN998275	RL_14Mar_13	Uncultured Syndiniales	Unknown	ES	Reloncaví Fjord, Chile	4
JN998276	RL_14Mar_14	Uncultured Syndiniales	Unknown	ES	Reloncaví Fjord, Chile	4
JN998277	RL_14Mar_15	Uncultured Syndiniales	Unknown	ES	Reloncaví Fjord, Chile	4
JN998278	RL_14Mar_16	Uncultured Syndiniales	Unknown	ES	Reloncaví Fjord, Chile	4
JN998279	RL_14Mar_17	Uncultured Syndiniales	Unknown	ES	Reloncaví Fjord, Chile	4
JN998280	RL_14Mar_18	Uncultured Syndiniales	Unknown	ES	Reloncaví Fjord, Chile	4
JN998281	RL_14Mar_19	Uncultured Syndiniales	Unknown	ES	Reloncaví Fjord, Chile	4
JN998282	RL_14Mar_20	Uncultured Syndiniales	Unknown	ES	Reloncaví Fjord, Chile	4
JN998283	RL_14Mar_21	Uncultured Syndiniales	Unknown	ES	Reloncaví Fjord, Chile	4
JN998284	RL_14Mar_22	Uncultured Syndiniales	Unknown	ES	Reloncaví Fjord, Chile	4
JN998285	RL_14Mar_23	Uncultured Syndiniales	Unknown	ES	Reloncaví Fjord, Chile	4
JN998286	RL_08Mar_01	Uncultured Syndiniales	Unknown	ES	Reloncaví Fjord, Chile	4
JN998287	RL_08Mar_02	Uncultured Syndiniales	Unknown	ES	Reloncaví Fjord, Chile	4
JN998288	RL_08Mar_03	Uncultured Syndiniales	Unknown	ES	Reloncaví Fjord, Chile	12
JN998289	RL_08Mar_04	Uncultured Syndiniales	Unknown	ES	Reloncaví Fjord, Chile	6
JN998290	RL_08Mar_05	Uncultured Syndiniales	Unknown	ES	Reloncaví Fjord, Chile	12
JN998291	RL_08Mar_06	Uncultured Syndiniales	Unknown	ES	Reloncaví Fjord, Chile	12
JN998292	RL_08Mar_07	Uncultured Syndiniales	Unknown	ES	Reloncaví Fjord, Chile	12
JN998293	RL_08Mar_08	Uncultured Syndiniales	Unknown	ES	Reloncaví Fjord, Chile	6
JN998294	RL_08Mar_09	Uncultured Syndiniales	Unknown	ES	Reloncaví Fjord, Chile	6
JN998295	RL_08Mar_10	Uncultured Syndiniales	Unknown	ES	Reloncaví Fjord, Chile	6
JN998296	RL_08Mar_11	Uncultured Syndiniales	Unknown	ES	Reloncaví Fjord, Chile	4
JN998297	RL_08Mar_12	Uncultured Syndiniales	Unknown	ES	Reloncaví Fjord, Chile	4
JN998298	RL_08Mar_13	Uncultured Syndiniales	Unknown	ES	Reloncaví Fjord, Chile	4
JN998299	RL_08Mar_14	Uncultured Syndiniales	Unknown	ES	Reloncaví Fjord, Chile	4
JN998300	RL_08Mar_15	Uncultured Syndiniales	Unknown	ES	Reloncaví Fjord, Chile	4
JN998301	RL_08Mar_16	Uncultured Syndiniales	Unknown	ES	Reloncaví Fjord, Chile	4
JN998302	RL_08Mar_17	Uncultured Syndiniales	Unknown	ES	Reloncaví Fjord, Chile	4
JN998303	RL_08Mar_18	Uncultured Syndiniales	Unknown	ES	Reloncaví Fjord, Chile	4
JN998304	RL_08Mar_19	Uncultured Syndiniales	Unknown	ES	Reloncaví Fjord, Chile	4
JN998305	RL_08Mar_20	Uncultured Syndiniales	Unknown	ES	Reloncaví Fjord, Chile	4
JN998306	RL_08Mar_21	Uncultured Syndiniales	Unknown	ES	Reloncaví Fjord, Chile	4
JN998307	RL_08Mar_22	Uncultured Syndiniales	Unknown	ES	Reloncaví Fjord, Chile	4
JN998308	RL_08Mar_23	Uncultured Syndiniales	Unknown	ES	Reloncaví Fjord, Chile	4
JN998309	RL_08Mar_24	Uncultured Syndiniales	Unknown	ES	Reloncaví Fjord, Chile	4
JN998310	RL_08Mar_25	Uncultured Syndiniales	Unknown	ES	Reloncaví Fjord, Chile	4
JN998311	RL_08Mar_26	Uncultured Syndiniales	Unknown	ES	Reloncaví Fjord, Chile	4
JN998312	RL_08Mar_27	Uncultured Syndiniales	Unknown	ES	Reloncaví Fjord, Chile	4